

1 Cell-based measurements to assess physiological status of *Pseudo-nitzschia multiseriata*, a
2 toxic diatom

3

4 Authors: Aurélie Lelong^a, Hélène Hégaret^a, Philippe Soudant^{a*}

5

6 ^aLEMAR (UMR6539), IUEM, Place Nicolas Copernic, 29280 Plouzané, France

7

8 aurelie.lelong@univ-brest.fr

9 helene.hegaret@univ-brest.fr

10 philippe.soudant@univ-brest.fr *Correspondance and reprints

11 Abstract

12 Diatoms of the genus *Pseudo-nitzschia* are potentially toxic microalgae, which blooms can
13 trigger Amnesic Shellfish Poisoning. The purpose of this study was to test and adapt different
14 probes and procedures to assess the physiological status of *Pseudo-nitzschia multiseriis* at the
15 cell-level, using flow cytometry. To perform these analyses, probes and procedures were first
16 optimized for concentration and incubation time. The percentage of dead *Pseudo-nitzschia*
17 cells, the metabolic activity of live cells and their intracellular lipid content were then
18 measured following a complete growth cycle. Additionally, chlorophyll autofluorescence and
19 efficiency of photosynthesis (quantum yield) were also monitored. The concentration and
20 viability of bacteria present in the medium were also assessed. Domoic acid (DA) was
21 quantified as well. Just before the exponential phase, cells exhibited a high metabolic activity,
22 but a low DA content. DA content per cell became most important at the beginning of the
23 exponential phase, when lipid storage was high, which provided a metabolic energy source,
24 and when they were surrounded with a high number of bacteria (high bacteria/*P. multiseriis*
25 ratio). These physiological measurements tended to decrease during exponential phase and
26 until stationary phase, where *P. multiseriis* cells did not content any DA nor stored any lipids
27 and started to die.

28

29 Keywords: flow cytometry; cell physiology; domoic acid; *Pseudo-nitzschia multiseriis*;
30 bacteria; fluorescent probes

31 1. Introduction

32 *Pseudo-nitzschia* is a potentially toxic diatom genus with a worldwide distribution.
33 Some species are able to produce domoic acid (DA), an amnesic shellfish toxin leading to
34 food poisoning (Sierra-Beltrán et al., 1998) with a few cases of mortality to humans (Wright
35 et al., 1989), plus hundreds of sea bird (Sierra-Beltrán et al., 1997, Work et al., 1993) or
36 marine mammal mortalities (Scholin et al., 2000, Fire et al., 2009, de la Riva et al., 2009).
37 These poisonings often occurred following a bloom of *Pseudo-nitzschia* spp. The reasons
38 why these blooms occurred are poorly known. Some studies tried to create models to predict
39 their occurrence (Anderson et al., 2009, Lane et al., 2009), but the determinism of each
40 bloom seems different. Although factors enhancing or decreasing *Pseudo-nitzschia* cell
41 toxicity have been intensively studied, they still remain unclear. The study of *Pseudo-*
42 *nitzschia* spp. physiology may help to understand why a bloom appears and becomes toxic.
43 Tools to assess the physiological status of microalgae are still fairly scarce. Photosynthetic
44 capacities of *Pseudo-nitzschia* spp. have been studied under different conditions (Ilyash et al.,
45 2007, El-Sabaawi and Harrison, 2006) but do not provide enough information to assess cell
46 physiological status. Besides photosynthetic parameters and chlorophyll content, others
47 parameters have sometimes been studied in diatoms, e.g. silicification (Leblanc et al., 2005,
48 Kroger and Poulsen, 2008) or carbohydrate levels (De Philippis et al., 2002, Magaletti et al.,
49 2004), but these are also insufficient to characterize the physiological processes occurring
50 inside the cell. It is therefore important to develop and then simultaneously measure several
51 different physiological parameters that may help to better understand the factors or status
52 associated with toxin production.

53

54 Assessment of cell physiology using fluorescent probes is a well-known subject in
55 medicine (Greenspan et al., 1985, Knot et al., 2005). Among the numerous fluorescent probes

56 available to assess cell physiology, some can be adapted to cultures of unicellular organisms.
57 They allow measurements of different physiological parameters such as metabolic activity
58 (with fluorescein diacetate, FDA), intracellular lipid content (Nile Red and BODIPY), total
59 DNA (SYBR Green) or mortality (SYTOX Green). Some of these probes have been used in
60 microalgal studies for several years but are often limited to microscopic observations or
61 spectrofluorimetric methods (Dempster and Sommerfeld, 1998, Okochi et al., 1999). The
62 latter allow measurement of an entire population, but differences between cells can not be
63 observed. Microscopic observations allow cell-by-cell analyses but are time consuming and
64 fluorescence quantification is difficult. On the other hand, flow cytometry (FCM) allows a
65 rapid analysis of the morphological and fluorescence characteristics of unicellular organisms
66 or individual cells. Even though FCM has a long history of routine use in medical analyses,
67 the first experiments to use FCM on microalgae were run only about thirty years ago (Olson
68 et al., 1983, Yentsch et al., 1983) and the approach still remains only a minor component for
69 measuring the physiology of phytoplankton. Some probes have already been tested on
70 microalgae using FCM, such as FDA (Dorsey et al., 1989, Brookes et al., 2000, Jochem,
71 1999), SYTOX Green (Veldhuis et al., 1997) or SYBR Green (Marie et al., 1997). Each of
72 these probes provides new insights for understanding how cells react under different
73 conditions, e.g. dark adaptation (Jochem, 1999), but they have never been applied
74 simultaneously to assess physiological status in a more comprehensive manner.

75
76 This study aims to assess the physiological status of *Pseudo-nitzschia multiseriis*
77 using a set of cell-based measurements. To reach this objective, different measurements were
78 developed and adapted to this species (i) to better understand its physiology under culture
79 conditions and (ii) to seek the relationship between the production of DA and cell
80 physiological status. The morpho-functional characteristics of *P. multiseriis* cells were

81 assessed by FCM, using different fluorescent probes (FDA, BODIPY 493/503, Nile Red,
82 SYTOX Green, SYBR Green and propidium iodide) and the measurement of chlorophyll
83 autofluorescence. Quantum yield (QY), which is a measurement of the efficiency of
84 photosynthesis, was measured using a pulse amplitude modulated (PAM) fluorometer.
85 Dissolved and particulate DA were measured on each culture using an ELISA assay. DA is a
86 secondary metabolite, thus supposed to be produced when cells have more energy than
87 necessary for the primary metabolism. Thus primary metabolism was assessed using FDA
88 and esterases activity. The availability of energy was assessed by measuring storage lipids, as
89 extra-energy is stored by microalgae under lipid form. The concentration of bacteria may
90 influence DA production by *P. multiseriis*, as they are known to enhance DA production
91 (Bates et al., 1995). Chlorophyll and QY measurements allow knowing if the culture is
92 healthy and were completed by the measure of dead cells percentage.

93 2. Materials and methods

94 2.1. Cultures

95 Strain CCAP 1061/32 of *Pseudo-nitzschia multiseriata* (isolated in 2007 in England)
96 was used for the experiments,. Cultures (n=6) were grown in sterilized f/2 medium (Guillard
97 and Hargraves, 1993) at 15.6°C ($\pm 0.2^\circ\text{C}$), and $131 \pm 16 \mu\text{mol photons m}^{-2} \text{s}^{-1}$ (light:dark
98 photoperiod of 12:12 h). Seawater used for f/2 medium was first filtered at 0.22 μm , to
99 eliminate any remaining bacteria (which was confirmed by flow cytometric measurements, as
100 described below) and then autoclaved. Cultures were xenic and grown without antibiotics.
101 Before each sampling, cultures were homogenized by gentle manual stirring. Almost all the
102 cells were present as single cells in our cultures; sometimes cells were forming 2 cells chains.
103 For the flow cytometry analysis, they were all considered as single cells.

104

105 2.2. Physiological measurements

106 Measurements were made with a FACScalibur flow cytometer (BD Biosciences, San
107 Jose, CA USA), using an argon blue laser (488 nm). Three fluorescence signals can be
108 detected by the flow cytometer: FL1 (green, 530 nm), FL2 (orange, 585 nm) and FL3 (red,
109 670 nm). Red fluorescence is linearly linked to the chlorophyll content of the cells and was
110 used as a discriminating characteristic to detect the microalgae (Fig. 1). Bacteria were
111 detected on the FL1 channel (Fig. 2), with different settings to those used for microalgae
112 analysis. Cell counts were estimated from the flow-rate measurement of the flow cytometer
113 (Marie et al., 1999) as all samples were run for 45 s. The flow rate from the FCM was
114 controlled every two days. Forward Scatter (FSC, light scattered less than 10 degrees) and
115 Side Scatter (SSC, light scattered at a 90 degree angle) were also measured. FSC is
116 commonly related to cell size and SSC to cell complexity. The same instrument settings were
117 used for the entire duration of the experiment to allow comparison between days.

118

119 *Bacteria.* Quantification of free-living bacteria in the *P. multiseriis* culture and the
120 percentage of dead bacteria in the culture were assessed by adding SYBR Green I (Molecular
121 probes, Invitrogen, Eugene, Oregon, USA) at a final concentration of 1/10000 of the
122 commercial solution, and propidium iodide (PI, Sigma, St. Louis, MO, USA) at 10 $\mu\text{g ml}^{-1}$ to
123 each sample. During analyses, aggregates of bacteria were taken into account with correction
124 according to aggregate size (Fig. 2). Bacterial counts were estimated as described for *Pseudo-*
125 *nitzschia* cells, using FL1 as a discriminating characteristic (due to SYBR Green fluorescence
126 staining).

127

128 *Mortality.* To assess *Pseudo-nitzschia* cell mortality, we used a cell membrane-
129 impermeable dye, SYTOX Green (Molecular probes, Invitrogen, Eugene, Oregon, USA)
130 prepared at a working solution of 5 μM . A mix of live/dead cells was prepared to confirm
131 that SYTOX Green stained only dead cells (Veldhuis et al., 2001) and to calibrate the
132 measurement. Cells from a dead culture (killed by heating for 15 min at 100°C) were mixed
133 with those from a live culture to give a range of 0 to 100% dead cells (increments of 10%)
134 and stained with SYTOX Green at 0.1 μM (final concentration) for 30 min. The percentage
135 of measured dead cells (those stained with SYTOX Green) was then compared to the
136 theoretical percentage of dead cells present in the mixture.

137

138 *Metabolic activity.* To assess metabolic activity, esterase activity was measured using
139 fluorescein diacetate (FDA, Molecular probes, Invitrogen, Eugene, Oregon, USA). FDA is a
140 probe that is cleaved by esterases inside the cells, resulting in fluorescein accumulation over
141 time (Jochem, 1999). A 5 mg ml^{-1} stock solution of FDA was prepared by diluting the
142 commercial powder in DMSO. A fresh 300 μM working solution was prepared before each

143 experiment by adding stock solution directly into distilled water cooled on ice. The working
144 solution was kept in darkness and on ice during the experiment and was agitated to prevent
145 the formation of aggregates.

146

147 *Lipids.* To assess the intracellular lipid content, two probes were tested on *P.*
148 *multiseriis*. A 10 mM stock solution of BODIPY 493/503 (4,4-difluoro-1,3,5,7,8-
149 pentamethyl-4-bora-3a,4a-diaza-s-indacene, Molecular probes, Invitrogen, Eugene, Oregon,
150 USA) was made by diluting the commercial powder in DMSO. A 1 mM working solution
151 was then prepared by a 10-fold dilution of the stock solution in distilled water. A 1 mg ml⁻¹
152 stock solution of Nile Red (NR, Sigma, St. Louis, MO, USA) was prepared by diluting 100-
153 fold the commercial powder in acetone and then 10-fold in distilled water to obtain a working
154 solution of 0.1 mg ml⁻¹.

155

156 Each of these measurements had to be optimized for *P. multiseriis*. Thus, final probe
157 concentrations and incubation times were chosen following two rules: (i) the concentration
158 had to be as low as possible to avoid toxic effects of the probe itself (and of the DMSO
159 contained in stock solutions of the probes) and (ii) the staining had to be homogeneous (all of
160 the cells had to be stained or only the dead cells for SYTOX Green), relatively stable over
161 time and reproducible between analytical replicates. For each probe, fluorescence
162 measurements were performed every 5 min during 1 h on the FL1 (or FL2 for NR) channel of
163 the flow cytometer. Concentrations of 0.5, 1.0, 2.5 and 5.0 µg ml⁻¹ were tested for NR; 1.0,
164 2.5, 5.0 and 10 µM for BODIPY; 0.75, 1.50 and 3.00 µM for FDA and 0.025, 0.05, 0.1 and
165 0.2 µM for SYTOX Green.

166

167 Quantum yield (QY), a measurement of the efficiency of photosynthesis, was
168 measured using an AquaPen-C AP-C 100 (Photo Systems Instruments, Czech Republic) pulse
169 amplitude modulated (PAM) fluorometer. $QY = (F_m - F_0)/F_m$, where F_0 and F_m are the
170 minimum and maximum fluorescence of cells, respectively, after 30 min of dark adaptation.
171 To ensure that there was no background fluorescence, *P. multiseriis* supernatant and f/2
172 medium were used as blanks.

173

174 Domoic acid (DA) was quantified using the ASP ELISA kit (Biosense Laboratories,
175 Bergen, Norway), according to the manufacturer's protocol. Cultures (cells and supernatant)
176 were sonicated and filtered at 0.22 μm to measure total DA. Supernatant (culture filtered at
177 0.22 μm) was used to measure dissolved DA. Intracellular DA was measured by subtracting
178 dissolved DA to total DA.

179

180 2.3. Monitoring the physiology of *P. multiseriis* over a growth cycle

181 Six *P. multiseriis* cultures of the same strain were sampled every day from day 4 to
182 21. The following were assessed on each sampling day: *P. multiseriis* morphology,
183 concentration and mortality, bacterial concentration and mortality, total and dissolved DA
184 concentrations, quantum yield, chlorophyll fluorescence, intracellular lipid content and
185 metabolic activity. Growth rate was measured during exponential phase following the
186 formula: $\mu \text{ (d}^{-1}\text{)} = \ln(N1/N0)/\Delta t$ (in days). Fluorescence measurements were performed using
187 the optimal concentrations obtained in the previous experiments: 0.1 μM SYTOX Green, 3
188 μM FDA, 1 $\mu\text{g ml}^{-1}$ Nile Red and 10 μM BODIPY. FDA measurements were performed
189 precisely after 6 min of incubation, and SYTOX Green and BODIPY measurements after 30
190 min. Bacteria were stained with SYBR Green and PI for 15 minutes.

191

192 2.4. *Statistics*

193 Results were analyzed statistically with simple regressions, One-Way ANOVA with
194 time as the main factor, as well as with principal component analysis (PCA) followed by a
195 factorial plan. For all statistical results, a probability of $p < 0.05$ was considered significant.
196 Statistical analyses were performed using StatGraphics Plus (Manugistics, Inc, Rockville,
197 MD, USA).

198

199 3. Results

200

201 3.1. Optimization of probe concentration

202 *Mortality.* A 0.1 μM final concentration of SYTOX Green allowed a good distinction
203 between dead and live cells (Fig. 1). Incubation time was optimal at 30 min. The best
204 correlation ($y=0.95x$, $R^2 = 0.99$, $P<0.01$) between the measured and theoretical percentages of
205 dead cells in the mixtures of dead/live *P. multiseriis* was established at a SYTOX Green
206 concentration of 0.1 μM , which was therefore applied for the further analyses.

207

208 *Bacteria.* Free-living bacteria are able to form aggregates that can be distinguished
209 after SYBR Green staining (Fig. 2A). Each aggregates exhibited a fluorescence that was
210 equivalent to the fluorescence of one bacteria x number of bacteria in the aggregate. The
211 number of total free-living bacteria can thus be deduced and measurements of FSC and SSC
212 can be done for each aggregate size (Fig. 2B).

213

214 *Metabolic activity.* Concentrations of FDA lower than 3.0 μM exhibited a low
215 fluorescence, indicating that there was little accumulation of the probe (data not shown). At
216 3.0 μM , fluorescein accumulated within the cells (Fig. 3I), in a linear manner during the 15
217 first min ($y=35.9x+133.1$, $R^2 = 0.9964$, $p<0.001$), and then reached a plateau (Fig. 4). For the
218 further analyses, fluorescein accumulation was measured after 6 min of staining within the
219 linear part of the curve.

220

221 *Lipids.* A final concentration of 10 μM BODIPY 493/503 and 1 $\mu\text{g ml}^{-1}$ of Nile Red
222 (NR) allowed the best staining of all cells (one distinct population of cells, not a diffuse cloud

223 of cells, can be seen on the cytograms, data not shown). After 30 min, all cells were well
224 stained and the fluorescence was stable (Fig. 3B, C, E, F).

225

226 3.2. Monitoring of morpho-functional characteristics during *P. multiseri* growth

227 The exponential growth phase of *P. multiseri* started after a 7-d lag phase, giving a
228 growth rate of $0.24 \pm 0.01 \text{ d}^{-1}$, and then the stationary phase was reached after day 17 (Fig. 5).
229 A maximal concentration of $\sim 8 \times 10^4 \text{ cells ml}^{-1}$ was observed at days 17 and 19, after which
230 the cell concentration rapidly declined.

231

232 Bacteria within the *P. multiseri* culture started their exponential growth phase on
233 day 7 and were still growing steadily until the end of the experiment (Table 1), exhibiting a
234 growth rate of $0.07 \pm 0.01 \text{ d}^{-1}$. The bacteria/*P. multiseri* cell ratio decreased during the
235 exponential phase of *P. multiseri*, remained stable between days 14 to 20, and then
236 increased again on the last day of the experiment, when *P. multiseri* numbers declined (Fig.
237 5, Table 1). Proportions of bacteria in aggregates of one, two or more cells did not change
238 with growth phases. The percentage of dead bacteria decreased between days 4 and 12 (from
239 $5.8\% \pm 0.6$ to $2.0\% \pm 0.2$) and then remained stable between 1.9 and 2.5% until day 21 (Table
240 1). Values of FSC and SSC for the bacterial community (free-living bacteria that were not
241 forming aggregates) decreased steadily during the course of *P. multiseri* culture (Table 1).

242

243 The percentage of dead *P. multiseri* cells averaged 28% throughout the entire
244 experiment (Table 1) and decreased from 30.3% on day 12 to 18.9% at day 16, after which it
245 increased to 43.8% on day 20 (stationary phase). FSC values for *P. multiseri* continuously
246 decreased during the experiment, almost linearly with culture age ($R^2=0.76$, $p<0.01$). SSC

247 values decreased until day 13 (mid-exponential phase) and became stable between day 13 and
248 the end of the experiment (Table 1).

249

250 Total DA in the *P. multiseriis* culture, expressed as pg ml^{-1} , increased steadily from
251 day 7 ($200 \pm 21 \text{ pg ml}^{-1}$) until day 14 ($798 \pm 164 \text{ pg ml}^{-1}$) during exponential growth. Total DA
252 in the culture then decreased sharply, reaching a concentration below 100 pg ml^{-1} on day 21.
253 Total DA content was highest on days 13 and 14, during the mid-exponential phase, and
254 decreased steadily after day 14, when it reached late-exponential phase and stationary phase
255 (Fig. 5). The amount of dissolved DA was low and remained constant throughout the culture,
256 from $41.3 (\pm 2.9) \text{ pg ml}^{-1}$ on day 6 to $103.0 (\pm 7.3) \text{ pg ml}^{-1}$ on day 12, representing 11 to 40 %
257 of total DA.

258

259 FL3 values (related to chlorophyll content) were measured on live cells, discriminated
260 from dead cells using SYTOX Green staining. FL3 values sharply decreased from day 4 to 6,
261 remained stable between days 6 (590 ± 12) and 9 (593 ± 10), and then slightly decreased from
262 day 9 to 20 (506 ± 12), stationary phase, Fig. 6). Quantum yield (QY) values increased
263 between days 5 (0.46 ± 0.01) and 8 (0.59 ± 0.01), became relatively stable until day 14
264 (0.62 ± 0.00), and then decreased in mid-exponential phase after day 14 (Fig. 6). Day 11
265 exhibited a significant decrease of both FL3 and QY. Supernatant and media did not exhibit
266 QY values or were below the detection threshold of the fluorometer.

267

268 The metabolic activity of the *P. multiseriis* cells, as measured with the FDA assay
269 after 6 min of incubation, increased rapidly from day 6 to 7 and then just as rapidly decreased
270 after day 7, to values just below the initial level, on day 9 (Fig. 7). The percentage of stained
271 cells after 6 min of incubation increased between day 8 ($72.5\% \pm 1.6$) and 16 ($87.9\% \pm 1.0$)

272 and decreased on day 20 ($74.7\% \pm 5.4$). The percentages of live cells, as measured with the
273 SYTOX Green and FDA assays, were significantly correlated, even though the correlation
274 remained quite weak ($R^2=0.67$ $p<0.001$, Fig. 7).

275

276 The amount of intracellular lipids, interpreted from BODIPY fluorescence, increased
277 between days 4 and 6, decreased from days 6 to 14 (during the exponential phase), stayed
278 stable until day 16, and finally increased during the stationary phase (Fig. 8). NR
279 fluorescence, the traditional indicator of lipid content, decreased between days 9 and 20, with
280 one higher fluorescence value on day 11 (Fig. 8).

281

282 PCA showed that DA content of cells (total DA) had coordinates really close to those
283 of Nile Red, SSC and bacteria/*Pseudo-nitzschia* ratio, knowing that components 1 and 2
284 explained 74 % of the variability (Fig. 9). FSC and BODIPY uptake were also closely
285 correlated with these previous parameters, indicating that increased DA production was
286 associated with a higher intracellular lipid content. A factorial plan (Fig. 10) was developed
287 from the previous PCA, plotting the age of the *P. multiseriis* culture, in exponential and
288 stationary phases from day 9 to 20. Days follow a consistent trend, from high component 1
289 and low component 2 (i.e. high lipid concentration, high DA content, high cell/bacteria ratio,
290 low esterases activity,) , towards lower component 1 and higher component 2 (i.e. high
291 esterases activity, low DA content and low lipid concentration, ...). Day 20 was the only days
292 which did not follow this trend, on the extremities of the factorial plan (extremely low
293 components 1 and 2, i.e. driven mainly by the high *P. multiseriis* mortality and high number
294 of bacteria).

295 4. Discussion

296 The first aim of this study was to test and optimize several methods and probes to
297 assess *Pseudo-nitzschia* physiological status. The percentage of cell mortality in the cultures
298 was determined using SYTOX Green, which only penetrates cells that have lost their
299 membrane integrity, and are thus considered as dead cells (Veldhuis et al., 1997). A final
300 concentration of 0.1 μM was optimal for staining *P. multiseriis* dead cells and is in good
301 agreement with those found in the literature for other phytoplankton species (Veldhuis et al.,
302 2001, Binet and Stauber, 2006, Ribalet et al., 2007, Miller-Morey and Van Dolah, 2004,
303 Lawrence et al., 2006).

304
305 Fluorescein diacetate (FDA) has previously been used to measure metabolic activity
306 (Jochem, 1999, Regel et al., 2002, Brookes et al., 2000) as well as viability of microalgae
307 (Lawrence et al., 2006, Dorsey et al., 1989, Jansen and Bathmann, 2007). It penetrates the
308 cells passively and once within the cell is hydrolyzed by non-specific esterases into
309 fluorescein and two acetate molecules. The more metabolically active the cells are, the more
310 esterases they produce, resulting in a greater amount of fluorescein accumulation within the
311 cells. The probe will not be cleaved within dead cells, as esterases are inactive. Moreover, if
312 the probe is hydrolyzed by any remaining esterases, the fluorescein will leak out of the cells,
313 as the membranes are permeable. Thus, unstained cells are considered as dead cells. In the
314 literature, measurement of fluorescein released from FDA inside the cells most often occurs
315 between 5 and 20 min of incubation (Jochem, 1999, Regel et al., 2002, Dorsey et al., 1989,
316 Jamers et al., 2009). FDA was only accumulated linearly during the first 15 to 20 min, as
317 previously observed by Gilbert et al. (1992). Accordingly, based on our results and supported
318 by the above publications, measurements were performed after 6 min of incubation. A final
319 concentration of 3 μM was optimal for this assay and is consistent with some publications

320 (Dorsey et al., 1989, Gilbert et al., 1992) but lower than others (Regel et al., 2002, Jamers et
321 al., 2009). Higher concentrations of FDA were not tested, as 3 μM provided satisfactory
322 staining and higher concentrations of FDA and DMSO may become toxic to the cells.

323

324 BODIPY 493/503 and Nile Red (NR) were tested to localize and quantify intracellular
325 lipids in *P. multiseriis* cells. NR has been used traditionally to stain lipids of microalgae
326 (Cooksey et al., 1987), whereas this is the first time that BODIPY 493/503 has been used to
327 study microalgal lipids. NR fluorescence of microalgal lipids, measured by FCM, has been
328 shown to be linearly correlated to the lipid content of cells (de la Jara et al., 2003). Lipids of
329 *P. multiseriis*, revealed by BODIPY and NR, were observed to form vacuoles inside the cells
330 (Fig. 3), and NR gave a lower fluorescence intensity than BODIPY. These vacuoles are likely
331 to contain reserve lipids, as BODIPY and NR are reported to stain neutral lipids (Gocze and
332 Freeman, 1994). Such vacuoles have previously been described within microalgae (Eltgroth
333 et al., 2005, Liu and Lin, 2001, Remias et al., 2009, Cooper et al., 2010), although lipid-
334 staining BODIPY and NR did not reveal a specific distribution of these vesicles. Both
335 BODIPY and NR were used to quantify intracellular lipid contents by FCM, in the green
336 (FL1) and orange (FL2) channels respectively. In the present study, NR was used at a final
337 concentration of 1 $\mu\text{g ml}^{-1}$, which is the same as used in previous studies on microalgae
338 (Chen et al., 2009, Chen et al., 2010, Liu et al., 2008, Huang et al., 2009, McGinnis et al.,
339 1997). BODIPY was used at a final concentration of 10 μM . This concentration allowed the
340 detection of subtle variations in the intracellular lipid content of *P. multiseriis* grown, for
341 example, in culture media with or without nitrate (data not shown), whereas lower
342 concentrations did not. Higher concentrations were not tested, as 10 μM provided satisfying
343 staining and higher concentrations of BODIPY and DMSO may become toxic to the cells.
344 The concentration used was 100 times higher than the one used for fungus (Saito et al., 2004)

345 but in agreement with those on human muscle (Wolins et al., 2001) and lower than the one
346 used on amoeba (Kosta et al., 2004).

347

348 The development of these methods allowed the physiological status of *P. multiseriis*
349 cells to be monitored over a complete growth cycle. The lag phase of *P. multiseriis* lasted 7
350 days, which is long compared to other studies on the same species, but not the same strain
351 (Thessen et al., 2009, Lundholm et al., 2004, Kudela et al., 2003, Kotaki et al., 1999, Bates et
352 al., 2000). The *P. multiseriis* growth rate ($0.24 \pm 0.01 \text{ d}^{-1}$) was lower than those previously
353 reported in the literature (Thessen et al., 2009, Lundholm et al., 2004, Kudela et al., 2003,
354 Kotaki et al., 1999, Bates et al., 2000). This might be explained by the age of the isolate
355 (isolated in 2007, more than 2 years ago) and the short cell length ($\sim 20 \mu\text{m}$); Amato et al.
356 (2005) reported a slight decrease in the growth rate of *P. delicatissima* with a decrease in
357 apical cell length. Culture conditions were the same or close to studies using *Pseudo-*
358 *nitzschia* cultures (media, irradiance and temperature) and thus could not explain differences
359 in growth rates.

360

361 FSC and SSC values of *P. multiseriis* decreased during the entire experiment, by 17%
362 and 22%, respectively. FSC and SSC result from the diffraction of the laser by the cell
363 surface. Their decrease in *P. multiseriis* may be related to changes in external morphology,
364 cell size and internal cell complexity. During growth, cells undergo asexual reproduction and
365 thus decrease in cell length. FSC and SSC values were, however, similar to values measured
366 over the last year (data not shown) at both the beginning (during the lag phase) and end of
367 experiments. This indicates that FSC and SSC values changed very little over the last year,
368 possibly because this strain isolated in 2007 was already quite old. Inoculation of *P.*
369 *multiseriis* into a new medium resulted in a return to high FSC and SSC values. Because

370 diatoms cannot increase their cell size, the changes in FSC and SSC values are more likely
371 related to both surface membrane and cytoplasmic modifications than cell size modifications,
372 thus modifying the diffraction of the laser. This hypothesis is based on the correlation
373 between SSC and both BODIPY and NR fluorescences ($R^2 = 0.77$ and 0.64 , respectively, at
374 $p < 0.01$). It may possible that when cells had a lot of lipid vesicles within their cytoplasm, this
375 increased cell complexity was reflected by the changes in FSC and SSC values.

376

377 Bacterial community counts and morphological changes within *Pseudo-nitzschia*
378 cultures were estimated for the first time by FCM. In this microalgal culture, the growth rate
379 of the bacteria was 0.07 d^{-1} , which remained constant over the course of the experiment; the
380 bacteria did not reach stationary phase during the 20 days of the experiment. This growth rate
381 is in the lower range of bacteria grown in adapted culture media, that can grow from 0.01 h^{-1}
382 (Kemp et al., 1993) to 1.5 h^{-1} (Makino et al., 2003). These differences may be due to the
383 competition with *P. multiseriis* for some nutrients or the fact that they may not have all the
384 nutrients they need and that are usually added in agar plates. The highest bacteria/*P.*
385 *multiseriis* ratios were measured during the lag phase (day 4 to 7) and at the beginning of the
386 exponential phase (day 7 and 8). Bacteria measured are the free-living bacteria contained in
387 the medium; however, some bacteria can also be attached directly to *P. multiseriis* cells
388 (Kaczmarska et al., 2005), these attached bacteria were not taken into account (their signal
389 was confounded within these of *P. multiseriis*). The decrease in the number of bacteria per *P.*
390 *multiseriis* cell during the exponential phase of *P. multiseriis* (from 922 to 180) is explained
391 by a faster growth rate of *P. multiseriis* compared to bacteria. The increase in the bacteria/*P.*
392 *multiseriis* ratio during the senescent phase of *P. multiseriis* may be a result of bacteria
393 taking advantage of organic materials released from dead *P. multiseriis* cells (Kaczmarska et
394 al., 2005). Stewart et al. (1997) found between 7 and 10 bacteria per *P. multiseriis* cell,

395 which is about 20 to 80 times lower than our values. This difference may be explained by (i)
396 a high residual percentage of dead *P. multiseriis* cells present during the entire experiment, or
397 (ii) the age of our isolate, which provided sufficient time (two years) for the bacterial
398 community to adapt to the culture conditions of *P. multiseriis*. Differences found in bacterial
399 communities over time in culture, for non-toxic *Pseudo-nitzschia pungens* support this
400 possibility (Sapp et al., 2007), but Wrabel and Rocap (2007) found no shifts in bacterial
401 assemblages in a *Pseudo-nitzschia* culture over its initial nine months (Wrabel and Rocap,
402 2007). Nevertheless, shift in the bacterial community may appear after 9 months in culture.
403 FSC and SSC values of the bacterial community decreased during the experiment. These
404 values are related to size and complexity of bacterial cells. This may reflect a shift in species
405 composition of the bacterial community to smaller bacteria or a decrease in bacterial cell size.
406 Between 1.9 and 5.8% of the bacteria in our cultures were dead, with the highest percentage
407 at day 4. The percentage of dead bacteria remained quite low (1.9-2.7%) until the end of the
408 experiment, as they were still in exponential phase.

409
410 Values of FL3 (related to the chlorophyll content) decreased slightly during the entire
411 experiment, with a greatest decrease between days 4 and 6. The chlorophyll content of *P.*
412 *multiseriis* decreased only slightly during the exponential phase. Nevertheless, cells with
413 more chlorophyll may not necessarily have the most efficient photosynthesis. Indeed, QY, a
414 measure of the efficiency of photosynthesis, was not well correlated to FL3 values, as QY
415 decreased during the stationary phase when FL3 remained high. QY increased at the
416 beginning of the exponential phase and remained high during the remaining exponential
417 phase, with cells having an efficient photosynthesis with a lot of energy produced. Such an
418 increase of QY during the exponential phase has been shown for other microalgal species,
419 e.g. *Symbiodinium* sp. (Rodriguez-Roman and Iglesias-Prieto, 2005), and is currently used as

420 a measure of algal culture health. As the QY value is not affected by the percentage of dead
421 cells in the cultures (Franklin et al., 2009), it can be speculated that at the end of the
422 stationary phase, live *P. multiseriis* cells still contained high amounts of chlorophyll, but with
423 a poor photosynthetic efficiency.

424

425 During the entire experiment, the percentage of dead *P. multiseriis* cells was
426 relatively high, ranging from 19% to 54%. Nevertheless, our cultures reached a maximum
427 cell concentration of 8×10^4 cells ml⁻¹, which is consistent with some previous studies
428 (Mengelt and Prézelin, 2002, Bates and Richard, 1996, Lewis et al., 1993, Kotaki et al., 1999)
429 but lower than the results of the majority of the studies (Bates and Richard, 1996, Kotaki et
430 al., 1999, Mengelt and Prézelin, 2002), suggesting that our cultures were not in good health,
431 which also explains the low growth rate and the high percentage of dead cells. Generally, in
432 healthy and young cultures of *Pseudo-nitzschia* sp., the percentage of dead cells has been
433 described under 5% (Mengelt and Prézelin, 2002). The increase in dead cells at the end of the
434 experiment may be due to the limitations in nutrients and associated with the beginning of the
435 stationary phase. Such a consistently high percentage of dead cells in the culture may be
436 explained by the age of the isolate. The percentage of dead cells assessed with FDA was
437 significantly but not perfectly correlated ($R^2 = 0.67$, $p < 0.01$) to those obtained with SYTOX
438 Green and appeared slightly lower than when measured with SYTOX Green. Cells can have a
439 compromised cell membrane, and be considered as dead when assessed with SYTOX Green,
440 but they may still have active esterases. These false-positive cells (dead but stained with
441 FDA) have been shown to represent 1.6% of total cells of *Chlamydomonas reinhardtii*
442 (Jamers et al., 2009). Such differences between SYTOX Green and FDA have also been
443 previously observed in *Heterosigma akashiwo* (Lawrence et al., 2006). Using these two
444 probes not only provides the percentage of dead versus live cells but also provides an

445 indication of the way cells are dying. In our cultures, cells most likely died by loss of
446 membrane integrity prior to inactivation of esterases, which was also observed by Lawrence
447 et al. (2006) in cultures of *H. akashiwo*. Thus, SYTOX Green and FDA provide useful
448 information and could both be used in physiological measurements.

449

450 Lipid-related fluorescence assessed with BODIPY was high during the lag phase,
451 indicating that the cells contained energy stored as neutral lipids. BODIPY fluorescence
452 decreased during the entire exponential phase, suggesting that cells were using these stored
453 lipids to grow, in addition to the energy produced by photosynthesis. Cells stopped growing
454 at the stationary phase, and energy was once again stored as lipids, as evidenced by the
455 increase in BODIPY fluorescence. Although no data are available between days 4 and 6, NR
456 fluorescence decreased during the remainder of the experiment, with the exception of a high
457 value on day 11. There was a weak correlation between BODIPY and NR fluorescence
458 during the exponential phase (between days 7 and 18; $R^2 = 0.65$, $p < 0.01$). During the
459 stationary phase, however, BODIPY fluorescence is higher than that of NR, which confirms
460 that these two probes may not actually stain the same compounds during that period. This
461 emphasises the importance of using both lipid probes. These differences may be explained by
462 the chemical properties of the two probes. BODIPY 493/503 stains intracellular lipids more
463 effectively than NR, with a higher sensitivity and lower background (Kacmar et al., 2006).
464 BODIPY 493/503 also stains intracellular lipid droplets more specifically than does NR
465 (Gocze and Freeman, 1994). NR is an uncharged hydrophobic molecule whose fluorescence
466 is strongly influenced by the polarity of its environment. As well as lipids, NR interacts with
467 many, but not all, native proteins (Sackett and Wolff, 1987) and can undergo changes in
468 fluorescence intensity when it binds to certain proteins (Brown et al., 1995). The fact that NR
469 binds proteins may explain its lower sensitivity to small variations in lipid content, as

470 measured by BODIPY. This is especially evident during the stationary phase, when
471 differences in lipid staining were observed between the two probes. Thus, the combined use
472 of BODIPY and NR probes is of interest as they may reflect different physiological changes.

473

474 The maximum of total DA per cell was observed on days 9 and 10, in early
475 exponential phase, and it decreased during the remainder of the exponential phase, and the
476 stationary phase. The same pattern of DA production has been observed for *Pseudo-nitzschia*
477 *calliantha* (Besiktepe et al., 2008) and *Pseudo-nitzschia pseudodelicatissima* (Pan et al.,
478 2001), where the maximum DA production was observed during the early exponential phase.
479 All studies of *P. multiseriis*, however, have found a maximum DA production during the
480 stationary phase (Kotaki et al., 1999, Bates et al., 2000, Lewis et al., 1993, Osada and
481 Stewart, 1997). Maybe old cultures of *P. multiseriis* exhibit a shift of DA production from
482 stationary phase to early exponential phase, which is difficult to prove, as one strain has
483 never been studied throughout its lifetime in laboratory. Moreover, strains exhibiting DA
484 production during early exponential phase seem to have a lower DA content per cell
485 (Besiktepe et al., 2008, Pan et al., 2001). In our study, total cellular DA varied between 0 and
486 192 fg cell⁻¹, which is low compared to previous studies on *P. multiseriis*, where DA attained
487 1.2 to 45 pg cell⁻¹ (Bates et al., 2000, Thessen et al., 2009). Our values are more consistent
488 with those of *P. calliantha* (Álvarez et al., 2009) or *P. pseudodelicatissima* (Pan et al., 2001),
489 which had a maximum toxicity of 10 and 36 fg cell⁻¹, respectively, but these species have a
490 smaller cell volume. Our strain of *P. multiseriis* was really short (around 20 µm length here,
491 whereas cells can be 100 µm long just after sexual reproduction, which may explain the low
492 values of DA it produced. DA intracellular content started to decrease from day 11 to the end
493 of the stationary phase. This decrease of DA may also coincide with a physiological stress.
494 Unfortunately, bacteria were not measured that day. Nevertheless, day 11 exhibited surprising
495 values of NR, FL3 and QY (i.e. out of the trend). Cells might have undergone a stress, with

496 loss of chlorophyll and thus decreased QY, thus energy was stored under lipid form and DA
497 production was stopped. Dissolved DA was particularly low but remained constant over time,
498 with cells excreting 11 to 40 % of their total DA. This low DA release may be due to the age
499 of the strain, isolated in 2007, and its consequent smaller size.

500

501 DA is a secondary metabolite and is thus believed to be produced when cells have
502 excess energy that is not used for primary metabolism (Bates, 1998). Meanwhile, extra
503 energy is stored as lipids when cells are not able to use it for primary metabolism. In this
504 study, the measure of FDA provided information regarding primary metabolism and QY
505 (photosynthetic efficiency) was measured to estimate the production of energy. There was no
506 clear relationship between DA production (total or dissolved) and QY or FDA hydrolysis.
507 Conversely, a positive correlation was observed between total DA content and NR after PCA
508 analysis (Fig. 9). Cells of *P. multiseriis* seemed to produce more DA when they had more
509 lipids, thus more available stored energy, which is in agreement with some studies (Whyte et
510 al., 1995) but not all (Pan et al., 1996). Indeed, Pan et al. (1996) made the hypothesis that DA
511 and lipid synthesis shared some precursors as Acetyl-CoA, so when DA is produced, lipids
512 can not be stored. Bacteria are also known to play a role in DA production, by enhancing DA
513 production through unknown mechanisms (Bates et al., 1995, Stewart et al., 1997). In this
514 study, the ratio of bacteria per *P. multiseriis* cell was also weakly correlated to DA content,
515 as the variable coordinates are quite close in the PCA analysis ($R^2=0.49$, $p<0.001$, Fig. 9).
516 Cells seemed to produce more DA when more bacteria per *P. multiseriis* cell were present in
517 the culture, possibly indicating that more DA was produced either when competition with
518 bacteria was greater or if bacteria produced toxin-enhancing compounds. FSC and BOPIDY
519 uptake were also closely correlated with DA content, SSC, NR and ratio bacteria/*Pseudo-*
520 *nitzschia*, indicating that increased DA content is associated with a higher intracellular lipid

521 content. This lipid increase can cause an increase in the amount and/or the size of lipid
522 vacuoles within the cells, which could also explain the increase observed in FSC and SSC of
523 the *P. multiseriis* cells. A factorial plan (Fig. 10) was developed from the previous PCA,
524 which plots the incubation time of the *P. multiseriis* culture, from day 9 to 20 (values
525 included in the previous PCA). The position of the days included on this factorial plan clearly
526 demonstrates and summarizes our findings: the gradual and continuous shift of the culture
527 from low algal concentration, high bacteria/algal ratio, large SSC, high lipid and DA content
528 in early stationary phase, towards increasing concentrations, reaching a maximum at the end
529 of the exponential phase, to finally showing a high percentage of dead algal cells and bacteria
530 in late stationary phase.

531

532 FCM has been previously used on microalgae, mainly to cell count or measure of only
533 one physiological parameter per experiment. Here, we developed a set of physiological
534 measurements, which provides a more complete description of the physiological status of the
535 microalgae. This technique has been applied to one species of *Pseudo-nitzschia* but can be
536 broadened to other microalgal species, whether or not they are toxic or diatoms. Developing
537 cell-based physiological measurements with FCM will help to further our understanding of
538 phytoplankton physiology and its responses to environmental changes, both biotic and
539 abiotic.

540

541 **Acknowledgements**

542 The authors would like to thank S.S. Bates for his constructive comments and English
543 corrections. This work was supported by the national program EC2CO MicrobiEN, the
544 “Région Bretagne” and the French ministry of research (MENRT grant).

545

546 **References**

547

548 Álvarez, G., Uribe, E., Quijano-Scheggia, S., López-Rivera, A., Mariño, C., Blanco, J., 2009.
549 Domoic acid production by *Pseudo-nitzschia australis* and *Pseudo-nitzschia calliantha*
550 isolated from North Chile. *Harmful Algae*.8,938-945.

551 Anderson, C. R., Siegel, D. A., Kudela, R. M., Brzezinski, M. A., 2009. Empirical models of
552 toxigenic *Pseudo-nitzschia* blooms: Potential use as a remote detection tool in the Santa
553 Barbara Channel. *Harmful Algae*.8,478-492.

554 Bates, S. S., (1998) Ecophysiology and metabolism of ASP toxin production. In:
555 Physiological ecology of harmful algal blooms. D. M. Anderson, A. D. Cembella and G. M.
556 Hallegraeff (eds). Springer-Verlag, Heidelberg, pp. 405-426.

557 Bates, S. S., Douglas, D. J., Doucette, G. J., Leger, C., 1995. Enhancement of domoic acid
558 production by reintroducing bacteria to axenic cultures of the diatom *Pseudo-nitzschia*
559 *multiseriis*. *Natural Toxins*.3,428-435.

560 Bates, S. S., Douglas, D. J., Doucette, G. J., Léger, C., 1995. Enhancement of domoic acid
561 production by reintroducing bacteria to axenic cultures of the diatom *Pseudo-nitzschia*
562 *multiseriis*. *Natural Toxins*.3,428-435.

563 Bates, S. S., Leger, C., Satchwell, M., Boyer, G. L., (2000) The effects of iron on domoic
564 acid production by *Pseudo-nitzschia multiseriis*. In: 9th International Conference on Harmful
565 Algal Blooms. G. A. Hallegraeff, S. I. Blackburn, C. J. Bolch and R. J. Lewis (eds). Hobart,
566 Tasmania: Intergov. Oceanogr. Comm., Paris, pp. 320–323.

567 Bates, S. S., Richard, J., (1996) Domoic acid production and cell division by *P. multiseriis* in
568 relation to a light: dark cycle in silicate-limited chemostat culture. In: 5th Canadian
569 Workshop on Harmful Marine Algae. . Canadian Technical Report of Fisheries and Aquatic
570 Sciences, pp. 140-143.

571 Besiktepe, S., Ryabushko, L., Ediger, D., Yimaz, D., Zenginer, A., Ryabushko, V., Lee, R.,
572 2008. Domoic acid production by *Pseudo-nitzschia calliantha* Lundholm, Moestrup et Hasle
573 (bacillariophyta) isolated from the Black Sea. *Harmful Algae*.7,438-442.

574 Binet, M. T., Stauber, J. L., 2006. Rapid flow cytometric method for the assessment of toxic
575 dinoflagellate cyst viability. *Marine Environmental Research*.62,247-260.

576 Brookes, J. D., Geary, S. M., Ganf, G. G., Burch, M. D., 2000. Use of FDA and flow
577 cytometry to assess metabolic activity as an indicator of nutrient status in phytoplankton.
578 *Marine and Freshwater Research*.51,817-823.

579 Brown, M. B., Miller, J. N., Seare, N. J., 1995. An investigation of the use of Nile Red as a
580 long-wavelength fluorescent probe for the study of alpha(1)-acid glycoprotein drug
581 interactions. *Journal of Pharmaceutical and Biomedical Analysis*.13,1011-1017.

582 Chen, W., Sommerfeld, M., Hu, Q., 2010. Microwave-assisted Nile red method for in vivo
583 quantification of neutral lipids in microalgae. *Bioresource Technology*.In Press, Corrected
584 Proof.

585 Chen, W., Zhang, C., Song, L., Sommerfeld, M., Hu, Q., 2009. A high throughput Nile red
586 method for quantitative measurement of neutral lipids in microalgae. *Journal of*
587 *Microbiological Methods*.77,41-47.

588 Cooksey, K. E., Guckert, J. B., Williams, S. A., Callis, P. R., 1987. Fluorometric
589 determination of the neutral lipid content of microalgal cells using Nile Red. *Journal of*
590 *Microbiological Methods*.6,333-345.

591 Cooper, M. S., Hardin, W. R., Petersen, T. W., Cattolico, R. A., 2010. Visualizing "green oil"
592 in live algal cells. *Journal of Bioscience and Bioengineering*.109,198-201.

- 593 de la Jara, A., Mendoza, H., Martel, A., Molina, C., Nordstron, L., de la Rosa, V., Diaz, R.,
594 2003. Flow cytometric determination of lipid content in a marine dinoflagellate,
595 *Cryptothecodinium cohnii*. Journal of Applied Phycology.15,433-438.
- 596 de la Riva, G. T., Johnson, C. K., Gulland, F. M. D., Langlois, G. W., Heyning, J. E., Rowles,
597 T. K., Mazet, J. A. K., 2009. Association of an unusual marine mammal mortality event with
598 *Pseudo-nitzschia* spp. blooms along the southern California coastline. Journal of Wildlife
599 Diseases.45,109-121.
- 600 De Philippis, R., Sili, C., Faraloni, C., Vincenzini, M., 2002. Occurrence and significance of
601 exopolysaccharide-producing cyanobacteria in the benthic mucilaginous aggregates of the
602 Tyrrhenian Sea (Tuscan Archipelago). Annals of Microbiology.52,1-11.
- 603 Dempster, T. A., Sommerfeld, M. R., 1998. Effects of environmental conditions on growth
604 and lipid accumulation in *Nitzschia communis* (Bacillariophyceae). Journal of
605 Phycology.34,712-721.
- 606 Dorsey, J., Yentsch, C. M., Mayo, S., McKenna, C., 1989. Rapid analytical technique for the
607 assessment of cell metabolic-activity in marine microalgae. Cytometry.10,622-628.
- 608 El-Sabaawi, R., Harrison, P. J., 2006. Interactive effects of irradiance and temperature on the
609 photosynthetic physiology of the pennate diatom *Pseudo-nitzschia granii* (Bacillariophyceae)
610 from the northeast subarctic Pacific. Journal of Phycology.42,778-785.
- 611 Eltgroth, M. L., Watwood, R. L., Wolfe, G. V., 2005. Production and cellular localization of
612 neutral long-chain lipids in the haptophyte algae *Isochrysis galbana* and *Emiliania huxleyi*.
613 Journal of Phycology.41,1000-1009.
- 614 Fire, S. E., Wang, Z., Leighfield, T. A., Morton, S. L., McFee, W. E., McLellan, W. A.,
615 Litaker, R. W., Tester, P. A., et al., 2009. Domoic acid exposure in pygmy and dwarf sperm
616 whales (*Kogia* spp.) from southeastern and mid-Atlantic U.S. waters. Harmful Algae.8,658-
617 664.
- 618 Franklin, D. J., Choi, C. J., Hughes, C., Malin, G., Berges, J. A., 2009. Effect of dead
619 phytoplankton cells on the apparent efficiency of photosystem II. Marine Ecology-Progress
620 Series.382,35-40.
- 621 Gilbert, F., Galgani, F., Cadiou, Y., 1992. Rapid assessment of metabolic activity in marine
622 microalgae - Application in ecotoxicological tests and evaluation of water quality. Marine
623 Biology.112,199-205.
- 624 Gocze, P. M., Freeman, D. A., 1994. Factors underlying the variability of lipid droplet
625 fluorescence in MA-10 leydig tumor cells. Cytometry.17,151-158.
- 626 Greenspan, P., Mayer, E. P., Fowler, S. D., 1985. Nile red: a selective fluorescent stain for
627 intracellular lipid droplets. Journal of Cell Biology.100,965-973.
- 628 Guillard, R. R. L., Hargraves, P. E., 1993. *Stichochrysis immobilis* is a diatom, not a
629 chrysophyte. Phycologia.32,234-236.
- 630 Huang, G.-H., Chen, G., Chen, F., 2009. Rapid screening method for lipid production in alga
631 based on Nile red fluorescence. Biomass and Bioenergy.33,1386-1392.
- 632 Ilyash, L. V., Belevich, T. A., Ulanova, A. Y., Matorin, D. N., 2007. Fluorescence parameters
633 of marine plankton algae at the assimilation of organic nitrogen. Moscow University
634 Biological Sciences Bulletin.62,111-116.
- 635 Jamers, A., Lenjou, M., Deraedt, P., Van Bockstaele, D., Blust, R., de Coen, W., 2009. Flow
636 cytometric analysis of the cadmium-exposed green alga *Chlamydomonas reinhardtii*
637 (Chlorophyceae). European Journal of Phycology.44,541-550.
- 638 Jansen, S., Bathmann, U., 2007. Algae viability within copepod faecal pellets: evidence from
639 microscopic examinations. Marine Ecology-Progress Series.337,145-153.
- 640 Jochem, F. J., 1999. Dark survival strategies in marine phytoplankton assessed by cytometric
641 measurement of metabolic activity with fluorescein diacetate. Marine Biology.135,721-728.

- 642 Kacmar, J., Carlson, R., Balogh, S. J., Srienc, F., 2006. Staining and quantification of poly-3-
643 hydroxybutyrate in *Saccharomyces cerevisiae* and *Cupriavidus necator* cell populations
644 using automated flow cytometry. *Cytometry Part A*.69A,27-35.
- 645 Kaczmarek, I., Ehrman, J. M., Bates, S. S., Green, D. H., Léger, C., Harris, J., 2005.
646 Diversity and distribution of epibiotic bacteria on *Pseudo-nitzschia multiseriis*
647 (Bacillariophyceae) in culture, and comparison with those on diatoms in native seawater.
648 *Harmful Algae*.4,725-741.
- 649 Kemp, P. F., Lee, S., Laroche, J., 1993. Estimating the growth rate of slowly growing marine
650 bacteria from Rna content. *Applied and Environmental Microbiology*.59,2594-2601.
- 651 Knot, H. J., Laher, I., Sobie, E. A., Guatimosim, S., Gomez-Viquez, L., Hartmann, H., Song,
652 L. S., Lederer, W. J., et al., 2005. Twenty years of calcium imaging: Cell physiology to dye
653 for. *Molecular Interventions*.5,112-127.
- 654 Kosta, A., Roisin-Bouffay, C., Luciani, M. F., Otto, G. P., Kessin, R. H., Golstein, P., 2004.
655 Autophagy gene disruption reveals a non-vacuolar cell death pathway in *Dictyostelium*.
656 *Journal of Biological Chemistry*.279,48404-48409.
- 657 Kotaki, Y., Koike, K., Sato, S., Ogata, T., Fukuyo, Y., Kodama, M., 1999. Confirmation of
658 domoic acid production of *Pseudo-nitzschia multiseriis* isolated from Ofunato Bay, Japan.
659 *Toxicon*.37,677-682.
- 660 Kroger, N., Poulsen, N., 2008. Diatoms-From cell wall biogenesis to nanotechnology. *Annual*
661 *Review of Genetics*.42,83-107.
- 662 Kudela, R., Roberts, A., Armstrong, M., (2003) Laboratory analyses of nutrient stress and
663 toxin production in *Pseudo-nitzschia* spp. from Monterey Bay, California. In: *Harmful Algae*
664 2002. K. A. Steidinger, J. H. Landsberg, C. R. Tomas and V. G.A. (eds). Florida and Wildlife
665 Conservation Commission, Florida Institute of Oceanography, and Intergovernmental
666 Oceanographic Commission of UNESCO, pp. 136–138.
- 667 Lane, J. Q., Raimondi, P. T., Kudela, R. M., 2009. Development of a logistic regression
668 model for the prediction of toxigenic *Pseudo-nitzschia* blooms in Monterey Bay, California.
669 *Marine Ecology-Progress Series*.383,37-51.
- 670 Lawrence, J. E., Brussaard, C. P. D., Suttle, C. A., 2006. Virus-specific responses of
671 *Heterosigma akashiwo* to infection. *Applied and Environmental Microbiology*.72,7829-7834.
- 672 Leblanc, K., Hare, C. E., Boyd, P. W., Bruland, K. W., Sohst, B., Pickmere, S., Lohan, M. C.,
673 Buck, K., et al., 2005. Fe and Zn effects on the Si cycle and diatom community structure in
674 two contrasting high and low-silicate HNLC areas. *Deep-Sea Research Part I-Oceanographic*
675 *Research Papers*.52,1842-1864.
- 676 Lewis, N. I., Bates, S. S., McLachlan, J. L., Smith, J. C., (1993) Temperature effects on
677 growth, domoic acid production, and morphology of the diatom *Nitzschia pungens* f.
678 *multiseriis*. In: *Toxic Phytoplankton Blooms in the Sea*. T. J. Smayda and Y. Shimizu (eds).
679 Amsterdam (Netherlands): Elsevier Science Publishers B.V., pp. 601–606.
- 680 Liu, C. P., Lin, L. P., 2001. Ultrastructural study and lipid formation of *Isochrysis* sp
681 CCMP1324. *Botanical Bulletin of Academia Sinica*.42,207-214.
- 682 Liu, Z.-Y., Wang, G.-C., Zhou, B.-C., 2008. Effect of iron on growth and lipid accumulation
683 in *Chlorella vulgaris*. *Bioresource Technology*.99,4717-4722.
- 684 Lundholm, N., Hansen, P. J., Kotaki, Y., 2004. Effect of pH on growth and domoic acid
685 production by potentially toxic diatoms of the genera *Pseudo-nitzschia* and *Nitzschia*. *Marine*
686 *Ecology-Progress Series*.273,1-15.
- 687 Magaletti, E., Urbani, R., Sist, P., Ferrari, C. R., Cicero, A. M., 2004. Abundance and
688 chemical characterization of extracellular carbohydrates released by the marine diatom
689 *Cylindrotheca fusiformis* under N- and P-limitation. *European Journal of Phycology*.39,133-
690 142.

- 691 Makino, W., Cotner, J. B., Sterner, R. W., Elser, J. J., 2003. Are bacteria more like plants or
692 animals? Growth rate and resource dependence of bacterial C : N : P stoichiometry.
693 *Functional Ecology*.17,121-130.
- 694 Marie, D., Partensky, F., Jacquet, S., Vaulot, D., 1997. Enumeration and cell cycle analysis of
695 natural populations of marine picoplankton by flow cytometry using the nucleic acid stain
696 SYBR Green I. *Applied and Environmental Microbiology*.63,186.
- 697 Marie, D., Partensky, F., Vaulot, D., Brussaard, C., 1999. Enumeration of phytoplankton,
698 bacteria, and viruses in marine samples. *Current Protocols in Cytometry*.11.11.11-11.11.15.
- 699 McGinnis, K. M., Dempster, T. A., Sommerfeld, M. R., 1997. Characterization of the growth
700 and lipid content of the diatom *Chaetoceros muelleri*. *Journal of Applied Phycology*.9,19-24.
- 701 Mengelt, C., Prézelin, B. B., (2002) Dark survival and subsequent light recovery for *Pseudo-*
702 *nitzschia multiseries*. In: Harmful Algae 2002. K. A. Steidinger, J. H. Landsberg, C. R.
703 Tomas and G. A. Vargo (eds). Florida Fish and Wildlife Conservation Commission, Florida
704 Institute of Oceanography, and Intergovernmental Oceanographic Commission of UNESCO,
705 Paris, pp. 388-390.
- 706 Miller-Morey, J. S., Van Dolah, F. M., 2004. Differential responses of stress proteins,
707 antioxidant enzymes, and photosynthetic efficiency to physiological stresses in the Florida
708 red tide dinoflagellate, *Karenia brevis*. *Comparative biochemistry and physiology*.
709 *Toxicology & pharmacology : CBP*.138,493-505.
- 710 Okochi, M., Taguchi, T., Tsuboi, M., Nakamura, N., Matsunaga, T., 1999. Fluorometric
711 observation of viable and dead adhering diatoms using TO-PRO-1 iodide and its application
712 to the estimation of electrochemical treatment. *Applied Microbiology and*
713 *Biotechnology*.51,364-369.
- 714 Olson, R. J., Frankel, S. L., Chisholm, S. W., Shapiro, H. M., 1983. An inexpensive flow
715 cytometer for the analysis of fluorescence signals in phytoplankton - chlorophyll and DNA
716 distributions. *Journal of Experimental Marine Biology and Ecology*.68,129-144.
- 717 Osada, M., Stewart, J. E., 1997. Gluconic acid/gluconolactone: physiological influences on
718 domoic acid production by bacteria associated with *Pseudo-nitzschia multiseries*. *Aquatic*
719 *Microbial Ecology*.12,203-209.
- 720 Pan, Y. L., Parsons, M. L., Busman, M., Moeller, P. D. R., Dortch, Q., Powell, C. L.,
721 Doucette, G. J., 2001. *Pseudo-nitzschia* sp. cf. *pseudodelicatissima* - a confirmed producer of
722 domoic acid from the northern Gulf of Mexico. *Marine Ecology-Progress Series*.220,83-92.
- 723 Pan, Y. L., Subba Rao, D. V., Mann, K. H., 1996. Changes in domoic acid production and
724 cellular chemical composition of the toxigenic diatom *Pseudo-nitzschia multiseries* under
725 phosphate limitation. *Journal of Phycology*.32,371-381.
- 726 Regel, R. H., Ferris, J. M., Ganf, G. G., Brookes, J. D., 2002. Algal esterase activity as a
727 biomeasure of environmental degradation in a freshwater creek. *Aquatic Toxicology*.59,209-
728 223.
- 729 Remias, D., Holzinger, A., Lutz, C., 2009. Physiology, ultrastructure and habitat of the ice
730 alga *Mesotaenium berggrenii* (Zygnemaphyceae, Chlorophyta) from glaciers in the European
731 Alps. *Phycologia*.48,302-312.
- 732 Ribalet, F., Berges, J. A., Ianora, A., Casotti, R., 2007. Growth inhibition of cultured marine
733 phytoplankton by toxic algal-derived polyunsaturated aldehydes. *Aquatic Toxicology*.85,219-
734 227.
- 735 Rodriguez-Roman, A., Iglesias-Prieto, R., 2005. Regulation of photochemical activity in
736 cultured symbiotic dinoflagellates under nitrate limitation and deprivation. *Marine*
737 *Biology*.146,1063-1073.
- 738 Sackett, D. L., Wolff, J., 1987. Nile red as a polarity-sensitive fluorescent probe of
739 hydrophobic protein surfaces. *Analytical Biochemistry*.167,228-234.

- 740 Saito, K., Kuga-Uetake, Y., Saito, M., 2004. Acidic vesicles in living hyphae of an arbuscular
741 mycorrhizal fungus, *Gigaspora margarita*. *Plant and Soil*.261,231-237.
- 742 Sapp, M., Wichels, A., Gerdtts, G., 2007. Impacts of cultivation of marine diatoms on the
743 associated bacterial community. *Applied and Environmental Microbiology*.73,3117-3120.
- 744 Scholin, C. A., Gulland, F., Doucette, G. J., Benson, S., Busman, M., Chavez, F. P., Cordaro,
745 J., DeLong, R., et al., 2000. Mortality of sea lions along the central California coast linked to
746 a toxic diatom bloom. *Nature*.403,80-84.
- 747 Sierra-Beltrán, A. P., Cruz, A., Nunez, E., Del Villar, L. M., Cerecero, J., Ochoa, J. L., 1998.
748 An overview of the marine food poisoning in Mexico. *Toxicon*.36,1493-1502.
- 749 Sierra-Beltrán, A. P., Palafox-Urbe, M., Grajales-Montiel, J., Cruz-Villacorta, A., Ochoa, J.
750 L., 1997. Sea bird mortality at Cabo San Lucas, Mexico: Evidence that toxic diatom blooms
751 are spreading. *Toxicon*.35,447-453.
- 752 Stewart, J. E., Marks, L. J., Wood, C. R., Risser, S. M., Gray, S., 1997. Symbiotic relations
753 between bacteria and the domoic acid producing diatom *Pseudo-nitzschia multiseries* and the
754 capacity of these bacteria for gluconic acid/gluconolactone formation. *Aquatic Microbial
755 Ecology*.12,211-221.
- 756 Thessen, A. E., Bowers, H. A., Stoecker, D. K., 2009. Intra- and interspecies differences in
757 growth and toxicity of *Pseudo-nitzschia* while using different nitrogen sources. *Harmful
758 Algae*.8,792-810.
- 759 Veldhuis, M. J. W., Cucci, T. L., Sieracki, M. E., 1997. Cellular DNA content of marine
760 phytoplankton using two new fluorochromes: Taxonomic and ecological implications.
761 *Journal of Phycology*.33,527-541.
- 762 Veldhuis, M. J. W., Kraay, G. W., Timmermans, K. R., 2001. Cell death in phytoplankton:
763 correlation between changes in membrane permeability, photosynthetic activity, pigmentation
764 and growth. *European Journal of Phycology*.36,167-177.
- 765 Whyte, J. N. C., Ginther, N. G., Townsend, L. D., 1995. Formation of domoic acid and fatty
766 acids in *Pseudonitzschia pungens f multiseries* with scale of culture. *Journal of Applied
767 Phycology*.7,199-205.
- 768 Wolins, N. E., Rubin, D., Brasaemle, D. L., 2001. TIP47 associates with lipid droplets.
769 *Journal of Biological Chemistry*.276,5101-5108.
- 770 Work, T. M., Barr, B., Beale, A. M., Fritz, L., Quilliam, M. A., Wright, J. L. C., 1993.
771 Epidemiology of domoic acid poisoning in brown pelicans (*Pelecanus occidentalis*) and
772 Brandt's cormorants (*Phalacrocorax penicillatus*) in California. *Journal of Zoo and Wildlife
773 Medicine*.24,54-62.
- 774 Wrabel, M. L., Rocap, G., (2007) Specificity of bacterial assemblages associated with the
775 toxin-producing diatom, *Pseudo-nitzschia*. In: 4th Symposium on Harmful Algae in the U.S.
776 Woods Hole, MA, pp. 191.
- 777 Wright, J. L. C., Boyd, R. K., de Freitas, A. S. W., Falk, M., Foxall, R. A., Jamieson, W. D.,
778 Laycock, M. V., McCulloch, A. W., et al., 1989. Identification of domoic acid, a
779 neuroexcitatory amino-acid, in toxic mussels from eastern Prince Edward Island. *Canadian
780 Journal of Chemistry*.67,481-490.
- 781 Yentsch, C. M., Mague, F. C., Horan, P. K., Muirhead, K., 1983. Flow cytometric DNA
782 determinations on individual cells of the dinoflagellate *Gonyaulax tamarensis var excavata*.
783 *Journal of Experimental Marine Biology and Ecology*.67,175-183.
- 784
- 785

786 **Legends to figures**

787 Figure 1. Cytograms of 50/50 dead/live cells of *Pseudo-nitzschia multiseriis* stained with
 788 SYTOX Green. A. Cytogram of FSC and SSC (morphological parameters, expressed in
 789 arbitrary units, AU) of *P. multiseriis*. B. Cytogram of FL1 and FL3 fluorescence of *P.*
 790 *multiseriis*. FL1 is the green fluorescence due to SYTOX Green, FL3 is the red fluorescence
 791 due to chlorophyll (AU). R1 are unstained cells (considered as live cells, in red) and R2 are
 792 stained cells (considered as dead cells, in green).

793 Figure 2. Bacteria stained with SYBR Green and propidium iodide. A. Histogram of FL1
 794 (green) fluorescence of bacteria; 1 to 7 representing aggregates of 1 to 7 or more bacteria.
 795 FL1 is the green fluorescence due to SYBR Green. B. Cytograms of morphological
 796 parameters of bacteria (FSC and SSC, expressed in arbitrary units, AU). Each colour
 797 represents one aggregate size (light green=one bacteria, dark blue=2 bacteria, pink=3
 798 bacteria, light blue=4 bacteria, yellow=5 bacteria, red=6 bacteria, dark green=7 or more
 799 bacteria).

800 Figure 3. Photomicrographs of *Pseudo-nitzschia multiseriis* cells in white light (A, D, G),
 801 epifluorescence light with filter “BP 515/560 / BS 580 / LP 590” (B, E, H), and filter “BP
 802 450-490 / BS 510 / LP 515” (C, F, I). A, B, C) Cells stained with BODIPY. D, E, F) Cells
 803 stained with Nile Red. G, H, I) Cells stained with FDA. Scale bar=10 μm .

804 Figure 4. Green fluorescence of *Pseudo-nitzschia multiseriis* cells (in arbitrary units, AU)
 805 stained with 3.0 μM of fluorescein diacetate (FDA) and measured on FL1 detector of a flow
 806 cytometer (n=3, mean \pm SD).

807 Figure 5. A- *Pseudo-nitzschia multiseriis* growth curve (y-axis) and bacteria/*P. multiseriis*
 808 ratio (z-axis, n=6, mean \pm SE). The exponential growth phase of *P. multiseriis* is framed with
 809 a black-lined rectangle. B- Concentration of total and dissolved domoic acid (DA) in the
 810 whole culture (y-axis, pg ml^{-1}) and cellular DA in fg cell^{-1} (z-axis, n=6, mean \pm SE).
 811 Exponential growth phase of *P. multiseriis* is framed with a black-lined rectangle.

812 Figure 6. Chlorophyll fluorescence (FL3, in arbitrary units, AU, y-axis) and Quantum Yield
813 (QY, z-axis) of live *Pseudo-nitzschia multiseriis* cells as a function of culture age. FL3 was
814 measured using flow cytometry on live cells, as determined by SYTOX Green staining (n=6,
815 mean \pm SE). The exponential growth phase of *P. multiseriis* is framed with a black-lined
816 rectangle.

817 Figure 7. Fluorescein diacetate (FDA) uptake (FL1 fluorescence of live cells, y-axis) and
818 percentage of *Pseudo-nitzschia multiseriis* live cells stained by FDA (z-axis) and detected
819 using flow cytometer FL1 detector (n=6, mean \pm SE). Exponential growth phase of *P.*
820 *multiseriis* is framed with a black lined rectangle. Correlation between the percentages of live
821 cells measured with the SYTOX Green and FDA assays is indicated in the small graph (in
822 arbitrary units, AU).

823 Figure 8. Green and orange fluorescences of *Pseudo-nitzschia multiseriis* cells stained with
824 BODIPY 493/503 and Nile Red (indicators of lipid content) and detected by the FL1 (y-axis)
825 and FL2 (z-axis) detectors, respectively, on a flow cytometer, in arbitrary units (n=6, mean \pm
826 SE). Exponential growth phase of *P. multiseriis* is framed with a black lined rectangle.

827 Figure 9. Principal Component Analysis (PCA) plot of all physiological measurements
828 between days 9 and 20 (D9 to D20) of the *P. multiseriis* culture (n=52).

829 Figure 10. Factorial plan issued from the previous PCA and plotting days of culture of *P.*
830 *multiseriis*, from day 9 to day 20 (D9 to D20, n=52).

831

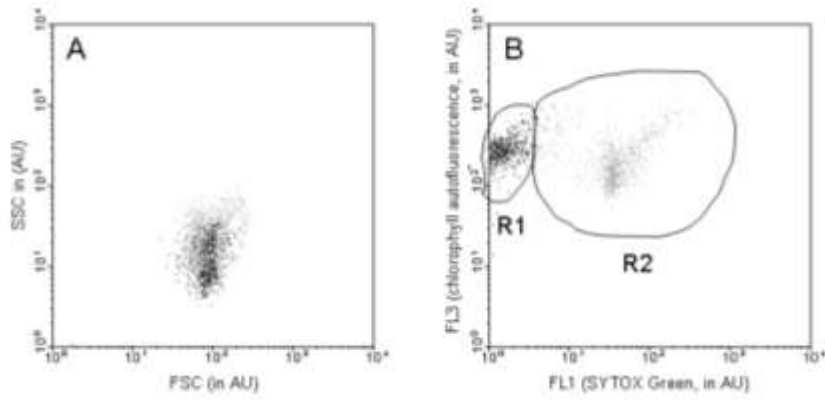
832 Table 1. *Pseudo-nitzschia multiseriis* and associated bacteria concentration (of live cells),
 833 morphological parameters (FSC and SSC, in arbitrary units), percentage of dead *P.*
 834 *multiseriis* measured using SYTOX Green and percentage of dead bacteria assessed using
 835 SYBR Green - propidium iodide double staining (n=6, mean \pm SE).

Day	<i>P. multiseriis</i>								Bacteria							
	FSC (AU)		SSC (AU)		% dead cells		Concentration (cell ml ⁻¹)		FSC (AU)		SSC (AU)		% dead cells		Concentration (10 ⁶ bact ml ⁻¹)	
	mean	\pm SE	mean	\pm SE	mean	\pm SE	mean	\pm SE	mean	\pm SE	mean	\pm SE	mean	\pm SE	mean	\pm SE
4	196.3	2.6	76.8	0.7	25.0	1.2	4 526	190	226.4	10.8	23.5	0.7	5.8	0.6	3.01	0.07
5	203.5	0.7	76.9	1.4	27.9	1.7	4 574	255	207.3	9.1	23.1	0.5	4.2	0.3	4.14	0.15
6	186.0	1.3	80.0	1.8	22.6	0.9	5 452	214	179.1	5.2	22.9	0.4	4.0	0.3	3.80	0.13
7	197.6	2.7	71.2	1.6	32.7	0.7	3 533	93								
8	183.7	2.9	72.6	1.5	30.6	0.8	6 226	275	177.4	2.8	23.0	0.2	3.5	0.3	5.61	0.04
9	185.2	1.5	72.1	1.0	32.6	2.0	7 711	677	179.1	4.6	24.5	0.3	2.6	0.3	5.33	0.23
10	190.5	2.0	67.5	1.3	28.5	2.7	9 059	1 179	168.9	7.5	24.3	0.4	2.7	0.2	5.15	0.20
11	190.5	1.6	62.9	0.7	54.5	9.4	12 393	1 730								2
12	186.3	1.4	63.3	0.9	30.3	3.8	15 863	2 716	127.6	5.0	23.2	0.4	2.0	0.2	6.09	0.21
13	180.4	1.3	59.1	0.8	22.8	3.0	23 837	5 343	186.5	18.7	23.0	1.5	1.9	0.1	6.60	0.12
14	177.4	2.0	58.7	1.1	22.9	2.9	30 726	6 223	171.4	26.7	20.2	0.6	2.2	0.2	6.80	0.21
15	173.5	0.9	59.7	1.3	19.1	0.7	33 796	4 967	193.3	7.7	21.1	0.7	2.2	0.1	7.71	0.23
16	171.1	1.9	60.0	1.3	18.9	1.6	36 148	2 064	225.9	18.1	22.7	1.4	2.2	0.1	8.19	0.16
17	185.4	0.9	57.3	1.2			77 322	3 718								
18	173.9	3.1	60.2	1.3	27.4	4.2	49 222	4 818	99.2	5.9	19.3	0.7	1.9	0.1	8.72	0.55
19	174.9	2.1	56.3	0.7			78 730	10 135								
20	168.8	1.3	60.3	0.3	43.8	5.5	55 889	8 682	177.9	8.6	19.0	0.7	2.0	0.1	11.31	0.97
21	163.7	2.3	59.7	0.5			40 163	2 226	25.1	0.7	17.3	0.4	2.1	0.2	13.30	0.81

836

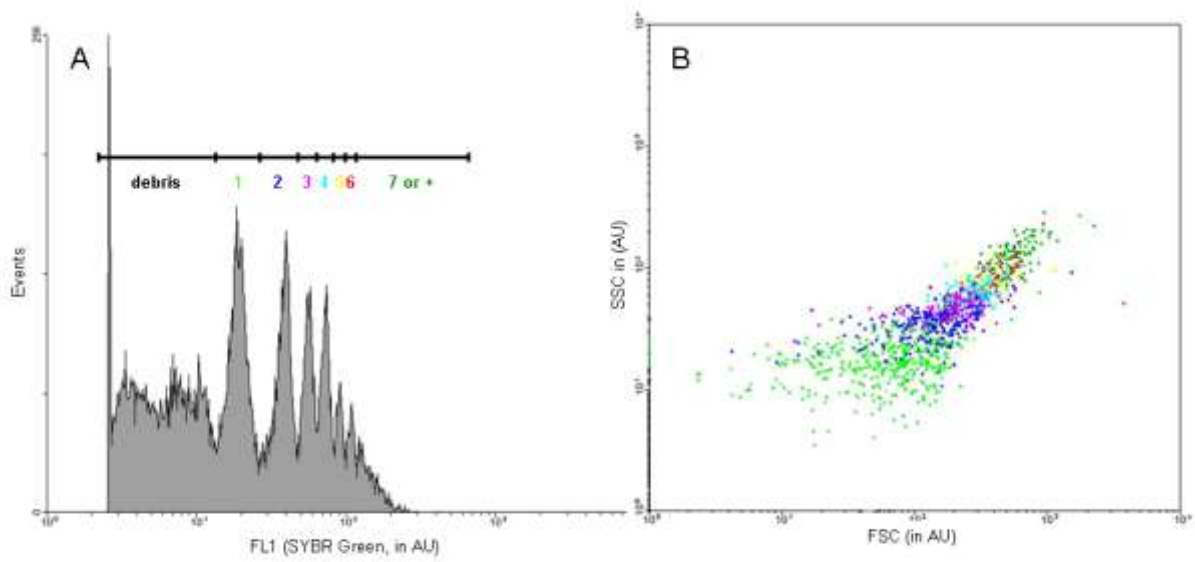
837 **Figures**

838 Fig. 1



839

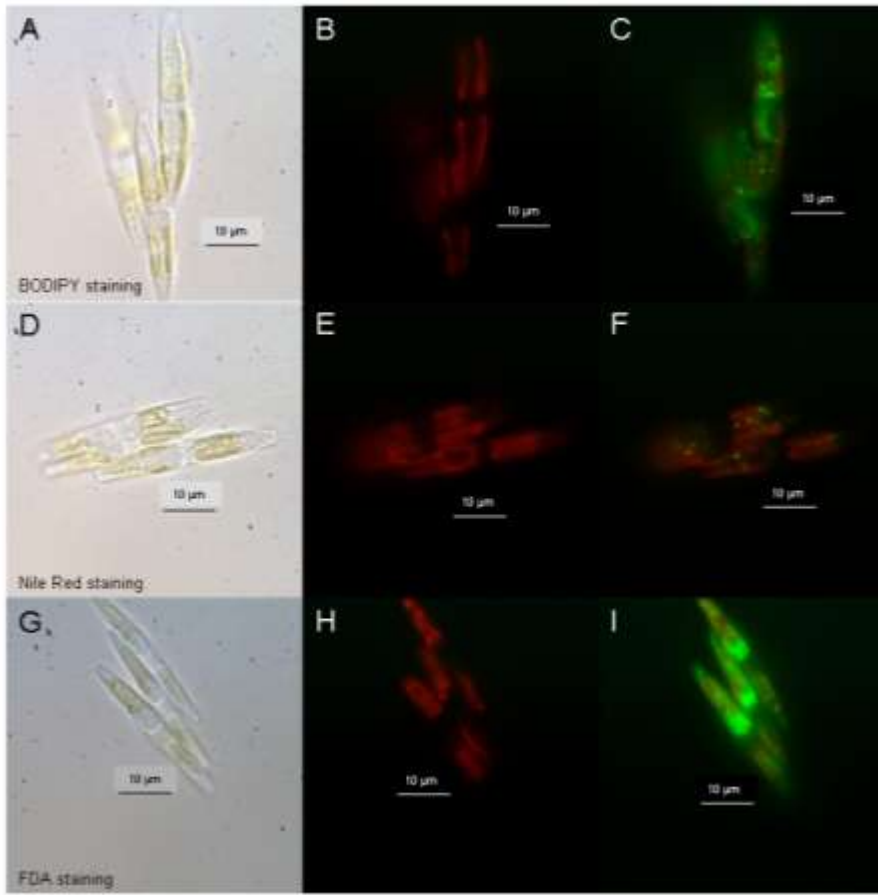
840 Fig. 2



841

842

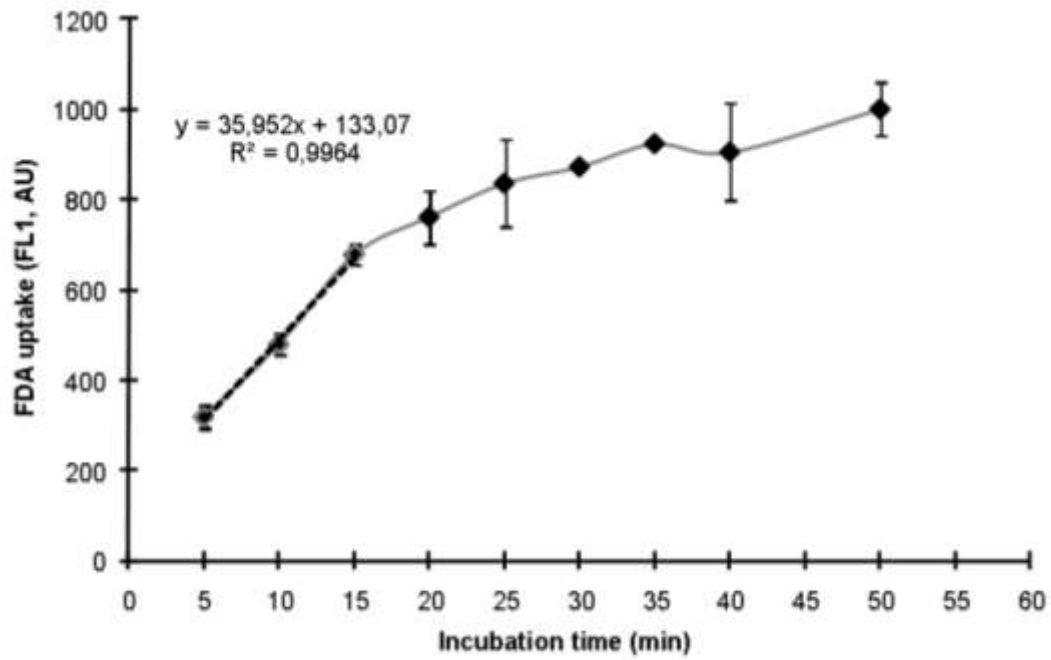
843 Fig. 3



844

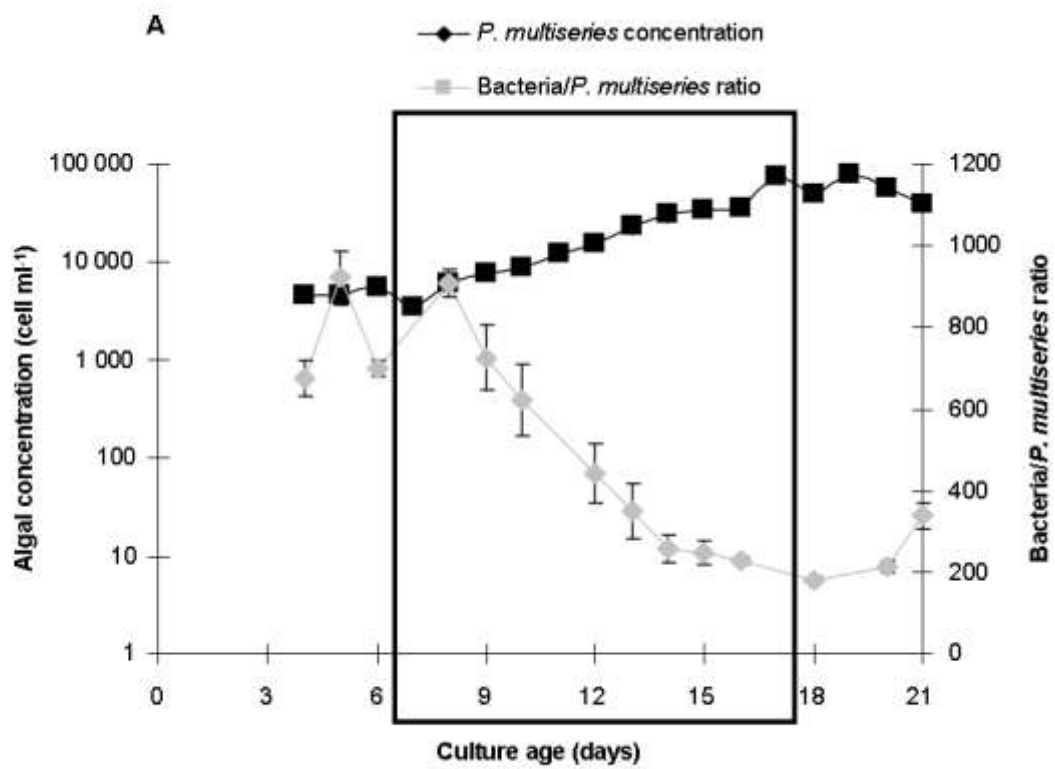
845

846 Fig. 4

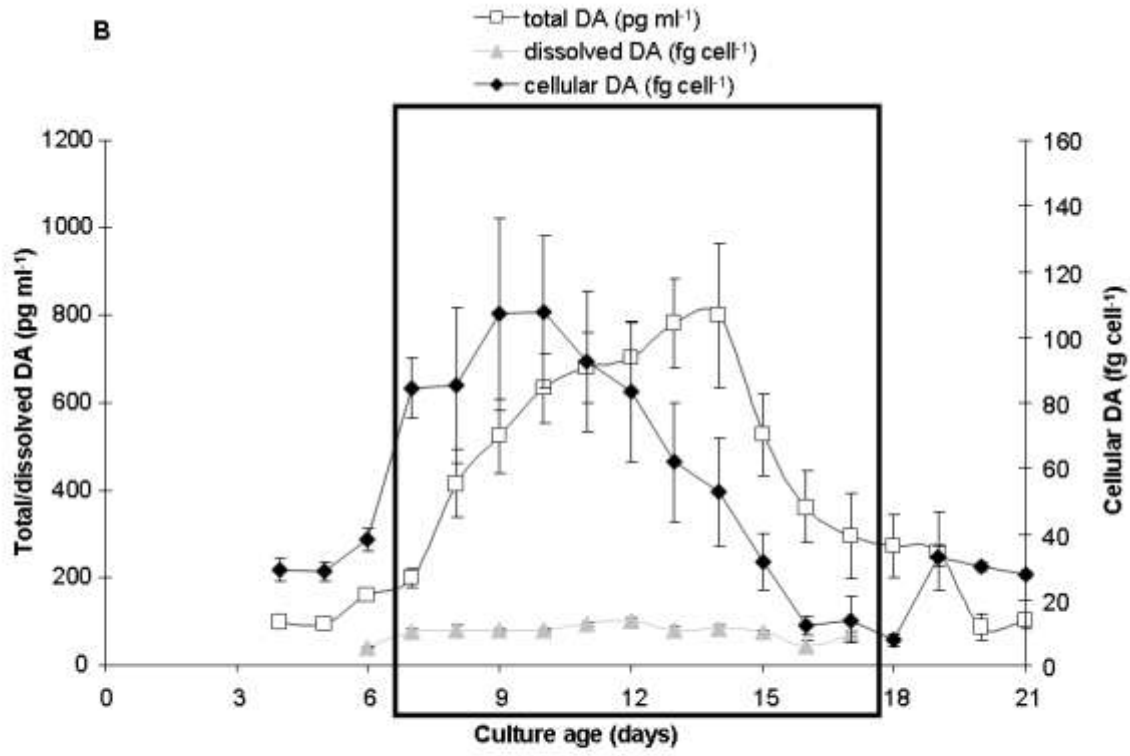


847

848 Fig. 5

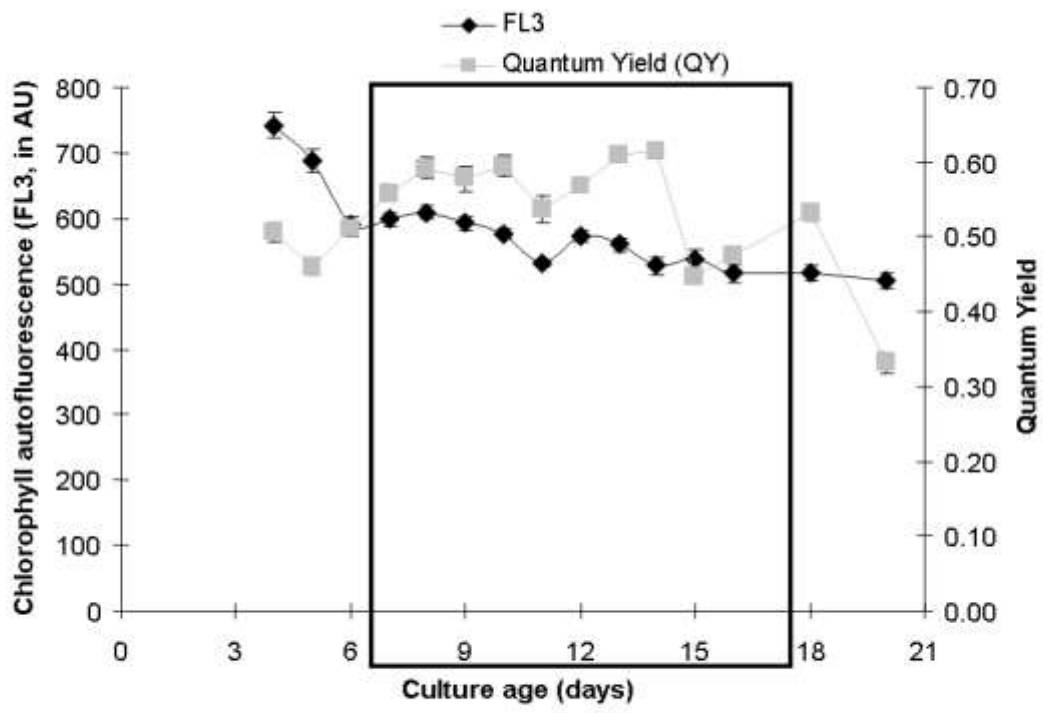


849



850

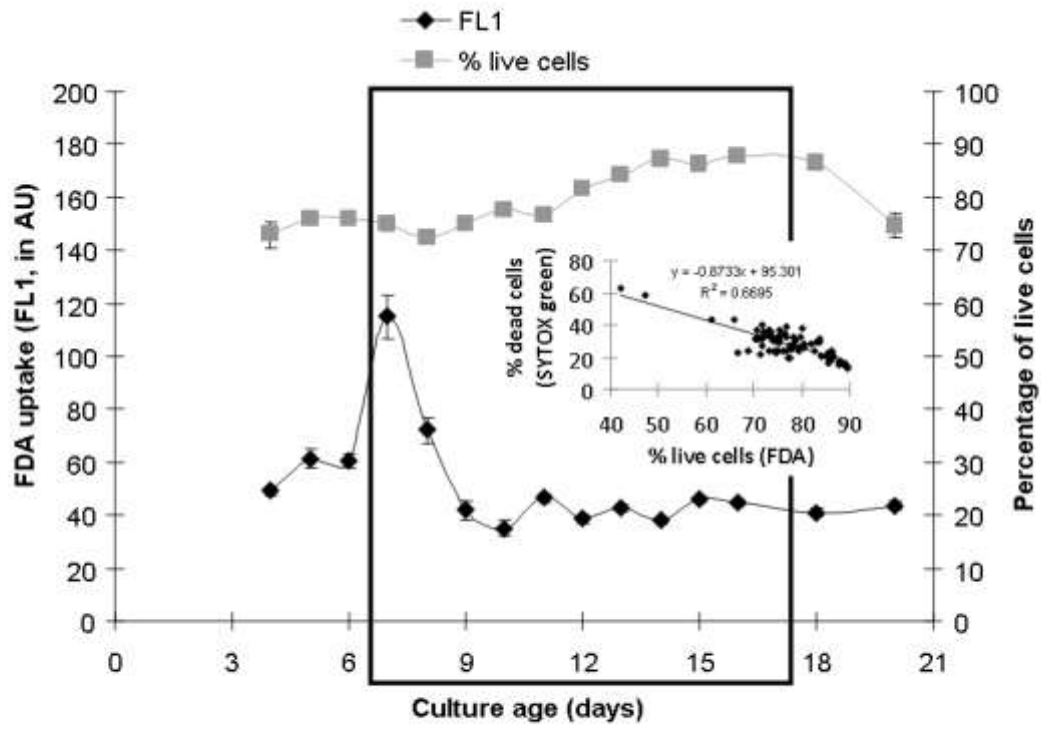
851 Fig. 6



852

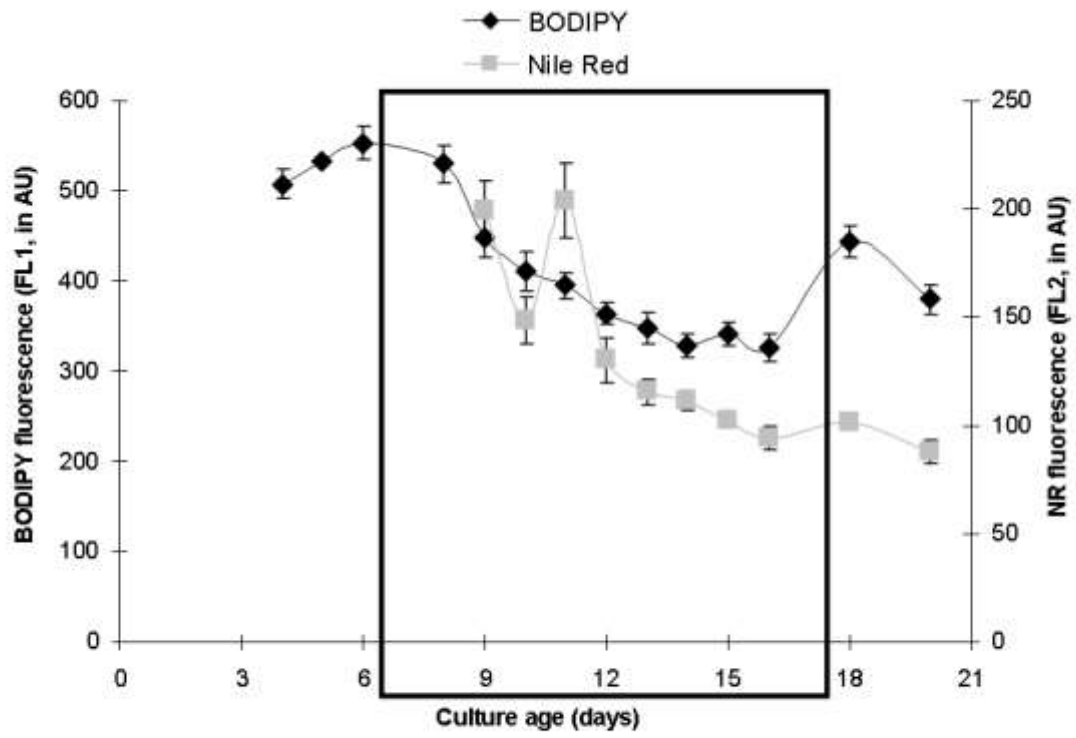
853

854 Fig. 7



855

856 Fig. 8



857

858 Fig. 9

859

860

861 Fig. 10

862